Supplemental Figure S1

A

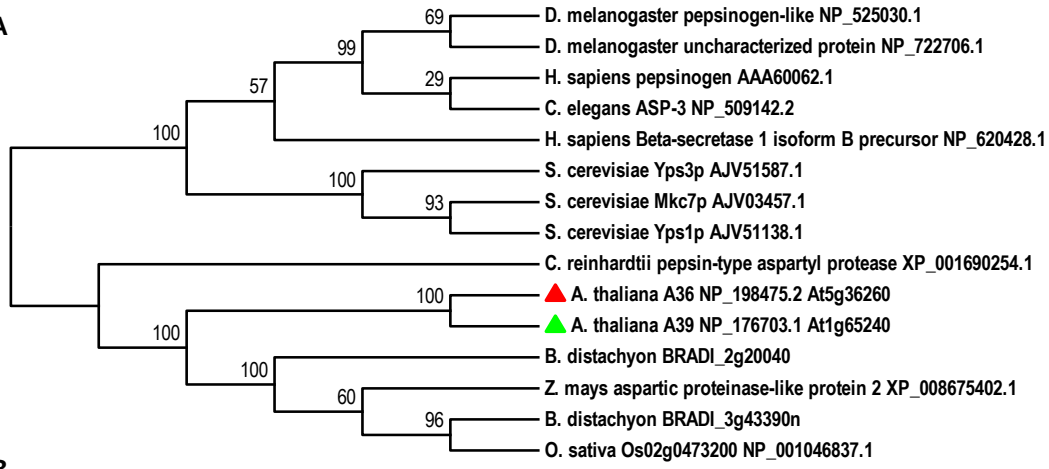

B

A36

Signal peptide

MVTTMDPSRISRIVAVVFVLVIQVVSGNFVFNVTHKFAGKEKQLSELKSHDSFRHARMLANIDLPLGGDS

RADSIGLYFTKIKLGSPPKEYYVQVDTGSDILWVNCAPCPKCPVKTDLGIPLSLYDSKTSSTSKNVGCED

DFCSFIMQSETCGAKKPCSYHVVYGDGSTSDGDFIKDNITLEQVTGNLRTAPLAQEVVFGCGKNQSGQL

ASP domain

GQTDSAVDGIMGFGQSNTSIISQLAAGGSTKRIFSHCLDNMNGGGIFAVGEVESPVVKTTPIVPNQVHYN

VILKGMDVDGDPIDLPPSLASTNGDGGTIIDSGTTLAYLPQNLYNSLIEKITAKQQVKLHMVQETFACFSFT

SNTDKAFPVVNLHFEDSLKLSVYPHDYLFSLREDMYCFGWQSGGMTTQDGADVILLGDLVLSNKLVVYD

transmembrane region

LENEVIGWADHNCSSSIKVKDGSGAAYQLGAENLISAASSVMNGTLVTLLSILIWVFHSFTS

A39

Signal peptide

MELRRKLCIVVAVFVIVIEFASANFVFKAQHKFAGKKKNLEHFKSHDTRRHSRMLASIDLPLGGDSRVDSV

GLYFTKIKLGSPPKEYHVQVDTGSDILWINCKPCPKCPTKTNLNFRLSLFDMNASSTSKKVGCDDDFCSF

ISQSDSCQPALGCSYHIVYADESTSDGKFIRDMLTLEQVTGDLKTGPLGQEVVFGCGSDQSGQLGNGD

ASP domain

SAVDGVMGFGQSNTSVLSQLAATGDAKRVFSHCLDNVKGGGIFAVGVVDSPKVKTTPMVPNQMHYNV

MLMGMDVDGTSLDLPRSIVRNGGTIVDSGTTLAYFPKVLYDSLIETILARQPVKLHIVEETFQCFSFSTNV

DEAFPPVSFEFEDSVKLTVYPHDYLFTLEEELYCFGWQAGGLTTDERSEVILLGDLVLSNKLVVYDLDNE

low complexity region

VIGWADHNCSSSIKIKDGSGGVYSVGADNLSSAPRLLMITKLLTILSPLIVMAFTSLA

C

```
A36          ....ADSIGLYFTKIKLGSPPKEYYVQVDTGSDILWVNCA     107
A39          ....VDSVGLYFTKIKLGSPPKEYHVQVDTGSDILWINCK     103
A3 (CDR1)    QIDLTSNSGEYLMNVSIGTPPFPIMAIADTGSDLLWTQCA     119
A35 (PCS1)   ............VTLTVGTPPQNISMVIDTGSELSWLRCN     102
Consensus                       g pp        dtgs   w  c
A36          DGDPIDLPPSLASTNGD..GGTIIDSGTTLAYLPQNLYNS     325
A39          DGTSLDLPRSIVRN.....GGTIVDSGTTLAYFPKVLYDS     318
A3 (CDR1)    GSKQIQYSGSDSESS.E..GNIIIDSGTTLTLLPTEFYSE     334
A35 (PCS1)   NGKLLPIPKSVLVPDHTGAGQTMVDSGTQFTFLLGPVYTA     319
Consensus              s          g    dsgt          y
```

Supplemental Figure S1. Evolutionary relationships of A36 and A39 amino acid sequences from Drosophila melanogaster (D. melanogaster), Homo sapiens (H. sapiens), Caenorhabditis elegans (C. elegans), Saccharomyces cerevisiae (S. cerevisiae), Chlamydomonas reinhardtii (C. reinhardtii), Arabidopsis thaliana (A. thaliana), Brachypodium distachyon (B. distachyon), Zea mays (Z. mays) and Oryza sativa (O. sativa). A, The evolutionary history was inferred using the Neighbor-Joining method by MEGA6.06. The bootstrap consensus tree inferred from 1000 replicates is taken to represent the evolutionary history of the taxa analyzed. The evolutionary distances were computed using the Poisson correction method and are in the units of the number of amino acid substitutions per site. The analysis involved 15 amino acid sequences. All positions containing gaps and missing data were eliminated. A36 is indicated by a red solid triangle. A39 is indicated by a green solid triangle. B, Protein structure domain analysis by SMART (http://smart.embl-heidelberg.de/) and the computer program SignalP version 2.0 (http://www.cbs.dtu.dk/services/SignalP-2.0/). The transmembrane region and ASP domain are indicated by the black line above the sequence row, which are predicted by SMART using the GENOMIC mode. The blue dotted box marked area are active sites. Prediction of potential C-terminal GPI-Modification Sites. Best predicted site is shown in red. Alternative site (second best) is shown in orange (http://mendel.imp.ac.at/gpi/gpi_server.html). C, Partial sequence alignment of A36, A39 and two other aspartic proteases A3 (CDR1) and A35 (PCS1) in the regions surrounding the active site.

Supplemental Figure S2

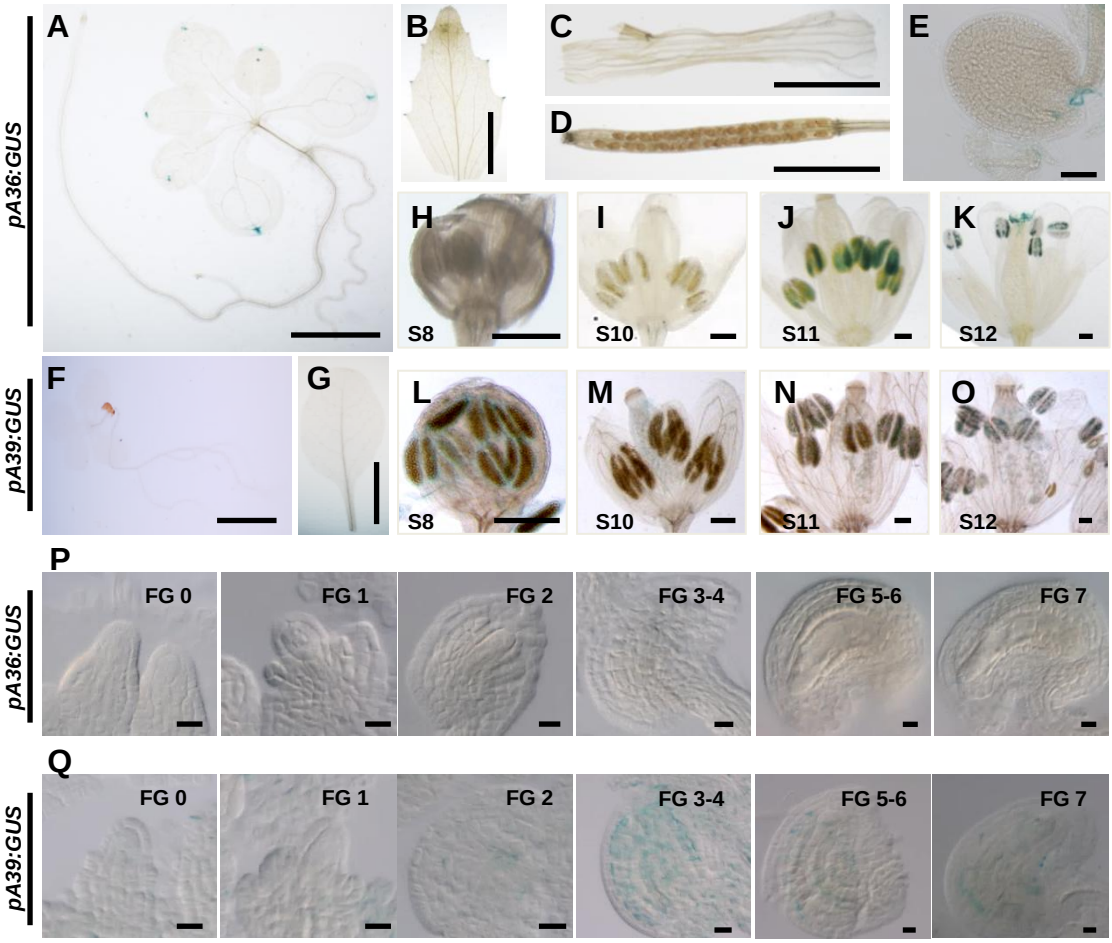

Supplemental Figure S2. Expression pattern of *A36* and *A39* by GUS staining. GUS staining analysis in transgenic plants of *pA36:GUS* showing the expression of *A36* in the seedling (A), leaf (B), stem (C) silique (D), ovule and pollen tube (E); Bars = 5 mm for (A and D), 1 cm for (B and C), 50 μm for (E). GUS staining analysis in transgenic plants of *pA39:GUS* showing the expression of *A39* in the seedling (F), leaf (G); Bars = 5 mm for (F and G). H to K, The expression of *A36* in developing flowers by GUS staining, flower at anther stage 8 (S8); flower at anther stage 10 (S10); flower at anther stage 11(S11); flower at anther stage 12 (S12). L to O, The expression anther of *A39* in developing flowers by GUS staining. H to O, Bars = 250 μm. Expression pattern of *A36* (P) and *A39*(Q) in the development of female gametophytes revealed by GUS staining. Bars = 10 μm.

Supplemental Figure S3

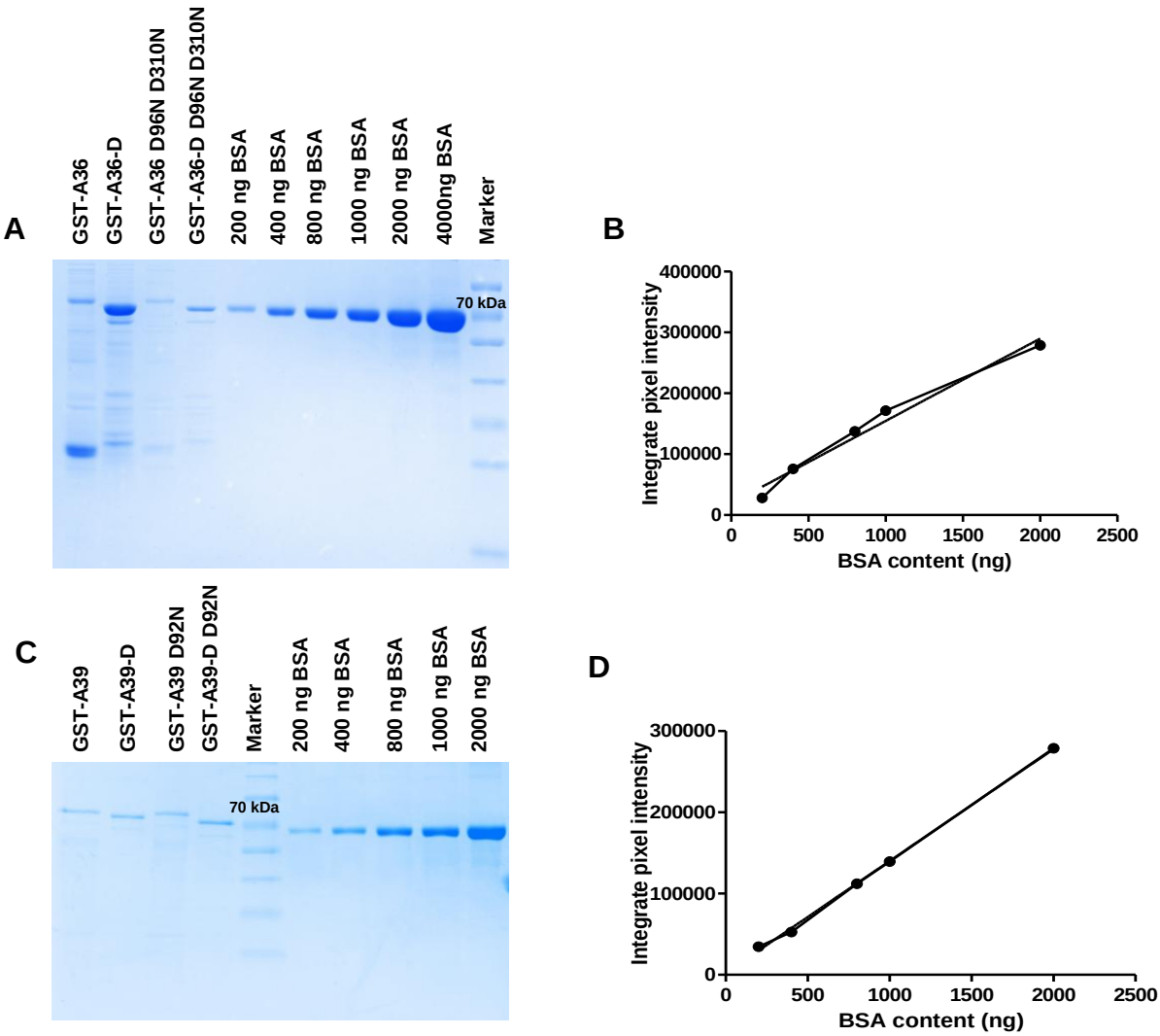

Supplemental Figure S3. Coomassie staining of purified GST-fusion proteins in SDS-PAGE and BSA standard curve. A, GST-A36 (79 kDa), GST-A36-D (72 kDa), GST-A36 D96N D310N (79 kDa), GST-A36-D D96N D310N (72 kDa) and BSA in different protein content (Albumin from bovine serum,66 kDa). B, The standard curve made by BSA in different protein content (200, 400, 800, 1000 ng, 2000 ng, 4000 ng) and corresponding mean gray value. The standard curve is calculated by Linear ($y = 1.56E\text{-}006 * x + 37.5$, $R^2 = 0.9796$). C, GST-A39 (78 kDa), GST-A39-D (70 kDa), GST-A39 D92N (78 kDa), GST-A39-D D92N (70 kDa) and BSA in different protein content (Albumin from bovine serum,66 kDa). D, The standard curve made by BSA in different protein content (200, 400, 800, 1000 ng, 2000 ng) and corresponding mean gray value. The standard curve is calculated by Linear ($y = 0.19E\text{-}006 * x - 80$, $R^2 = 0.99$).

Supplemental Figure S4

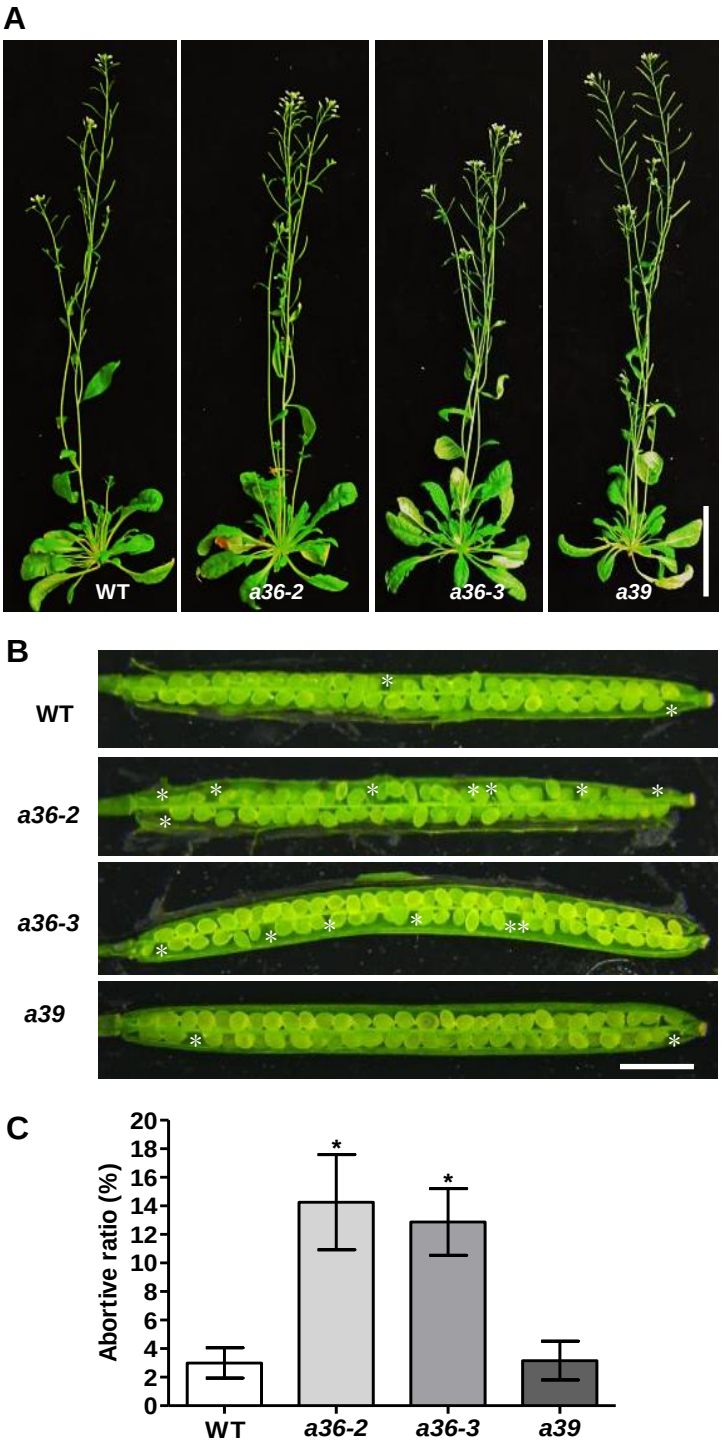

Supplemental Figure S4. The phenotype of the *a36* and *a39* single mutants. A, Phenotype comparison of 6-week-old plants between the wild-type and different allelic *a36* and *a39* mutants. Bar = 5 cm. B, The *a36-2* and *a36-3* mutation has reduced seed set. Asterisk designate unfertilized ovules in the silique. Bar = 2 mm. C, Statistical analysis for the abortive rates of seed sets. The values are based on three biological replicates (n = 300), where the error bars show the standard error and an asterisk indicates values that significantly differ from those of the wild-type (*P <0.05, calculated using One-way ANOVA).

Supplemental Figure S5

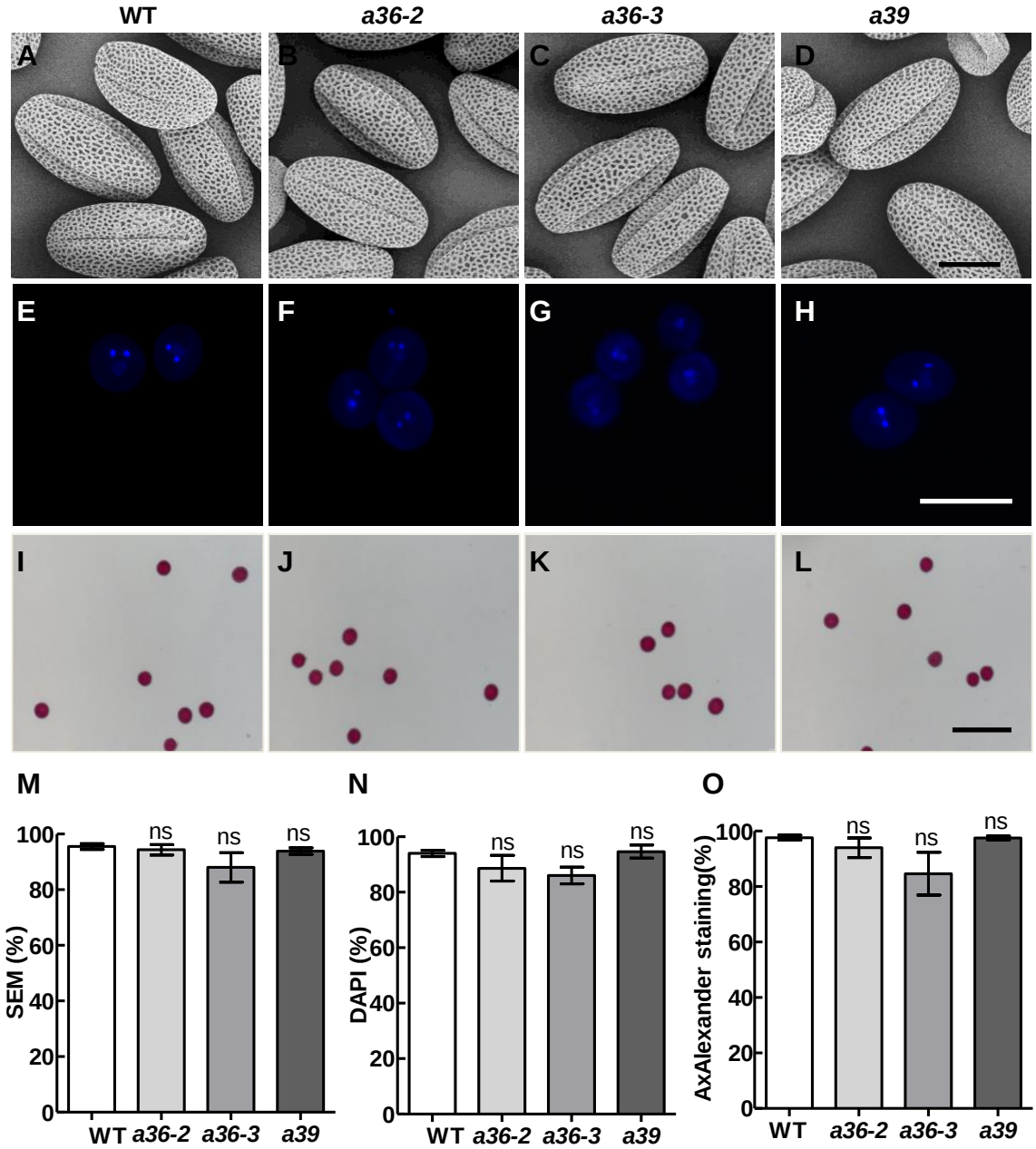

Supplemental Figure S5. SEM observation and staining of pollen grains from *a36* and *a39* mutant. A to D, SEM image of wild-type (A), *a36-2* (B), *a36-3* (C), *a39* (D) pollen grains. Bar = 10 μm. E to H, DAPI staining of pollen grains from wild-type (E), *a36-2* (F), *a36-3* (G), *a39* (H). Bar = 50 μm. I to L, Alexander staining from wild-type (I), *a36-2* (J), *a36-3* (K), *a39* (L). Bar = 100 μm. M, Statistical analysis of the normal pollen grains morphology by SEM. N, Statistical analysis of the pollen grains with normal nuclear morphology by DAPI staining. O, Statistical analysis of the pollen grains with normal cytoplasm morphology by Alexander staining. M to O, The data were collected from three independent experiments (n > 300). The error bars show the standard error (ns means no significant, calculated using One-way ANOVA).

Supplemental Figure S6

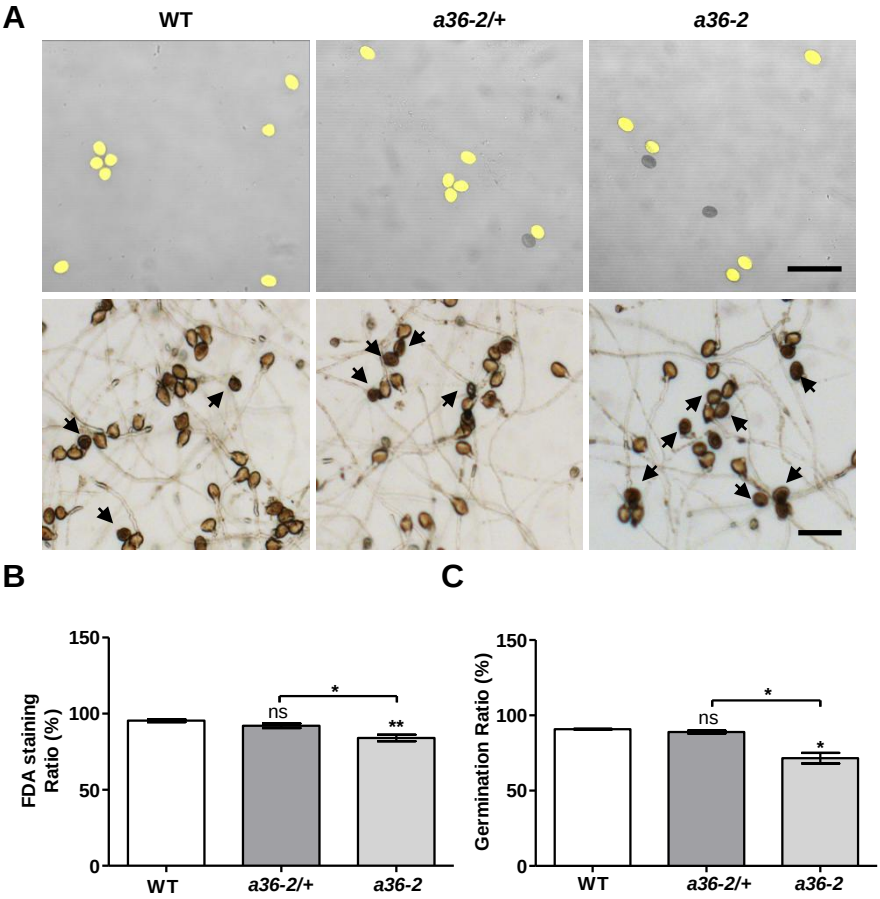

Supplemental Figure S6. *a36-2/+* displays slightly reduced pollen grain activity and pollen germination ratio *in vitro*. A, FDA staining (top row) and pollen germination assay (bottom row) in wild-type, *a36-2/+*, *a36-2*. FDA positive (viable) were indicated as yellow color. Pollens of wild-type, *a36-2/+*, *a36-2* germinated eight hours incubation *in vitro* (bottom row). Arrows designate ungerminated pollens. Bars = 100 μm. B and C, Statistical analysis of pollen viability by FDA staining (B) and germination rates (C) of pollen grains from wild-type, *a36-2/+*, *a36-2* plants *in vitro*. Data were collected from three independent experiments (n > 900). The error bars show the standard error and an asterisk indicates values that significantly differ from those of the wild-type (*$P < 0.05$, **$P < 0.01$, ns means no significant, calculated using Two-way ANOVA).

Supplemental Figure S7

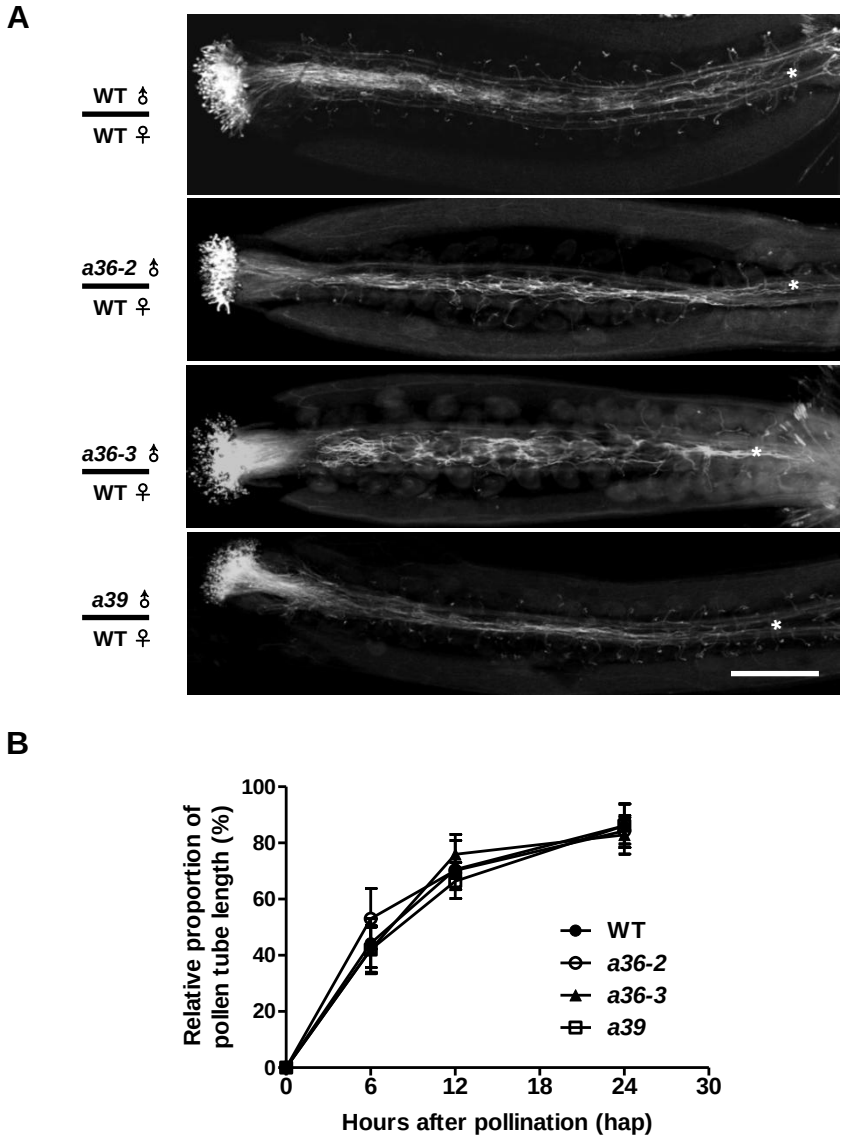

Supplemental Figure S7. Pollen tube growth of *a36* and *a39* mutants are normal in wild-type transmitting tract. A, Aniline blue staining of pollen tubes from wild-type, *a36-2*, *a36-3* and *a39* about 12 hours after pollination. The asterisk shows the location of the pollen tube. Bar = 2 mm. B, Statistical analysis of pollen tube length at different time points. Data were collected from three independent experiments(n = 135), the error bars show the standard error (calculated Two-way ANOVA).

Supplemental Figure S8

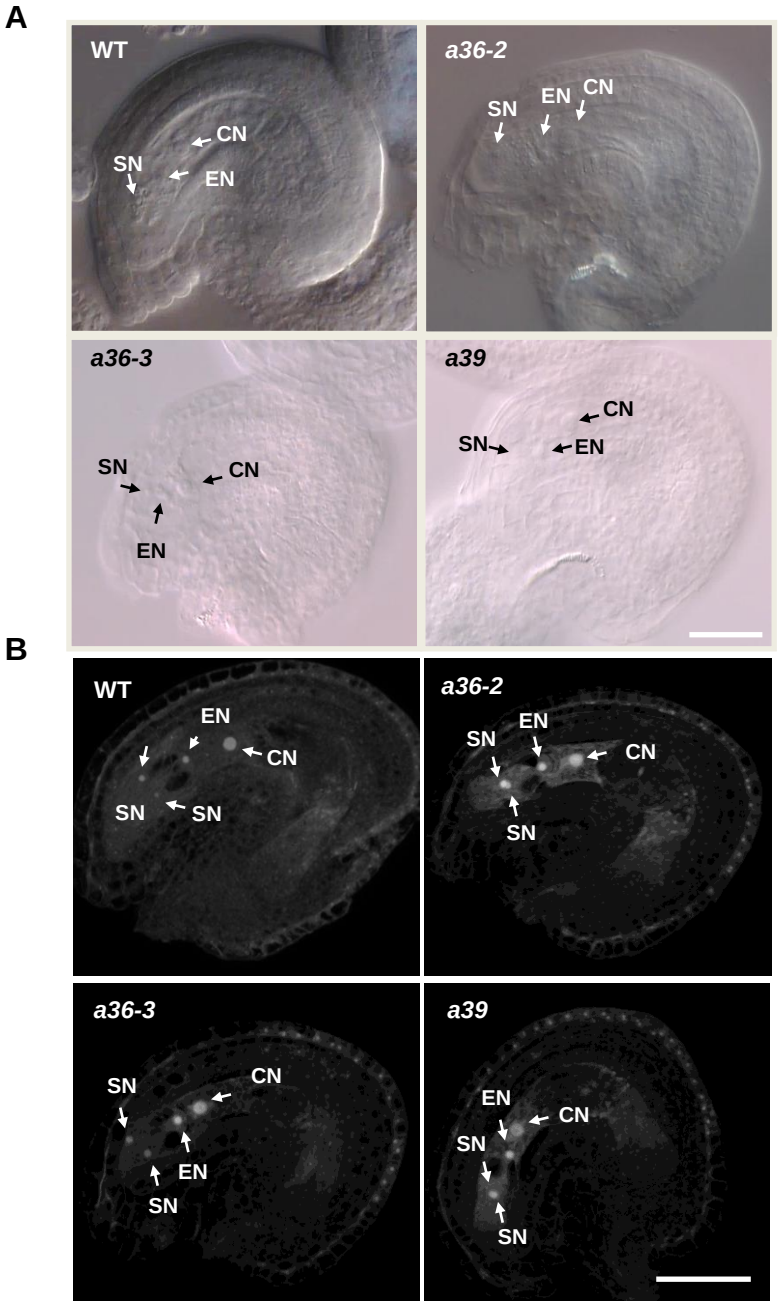

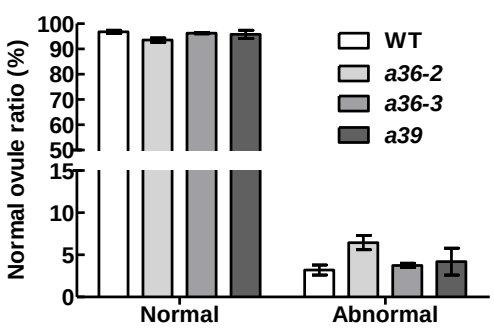

Supplemental Figure S8. Ovules with a mature seven-celled embryo sac at FG7 were observed by DIC and CLSM. A and B, Ovule with a mature seven-celled embryo sac at FG7 in the wild-type, *a36-2*, *a36-3* and *a39*, the embryo sac consists of two synergids nucleus (SN), the egg cell nucleus (EN), the large central cell nucleus (CN) by DIC (A) and CLSM (B). Bars = 20 μm. C, Statistical analysis of the normal ovule (FG7) ratio. Data were collected from three independent experiments (n = 600), the error bars show the standard error (Calculated using Two-way ANOVA).

Supplemental Figure S9

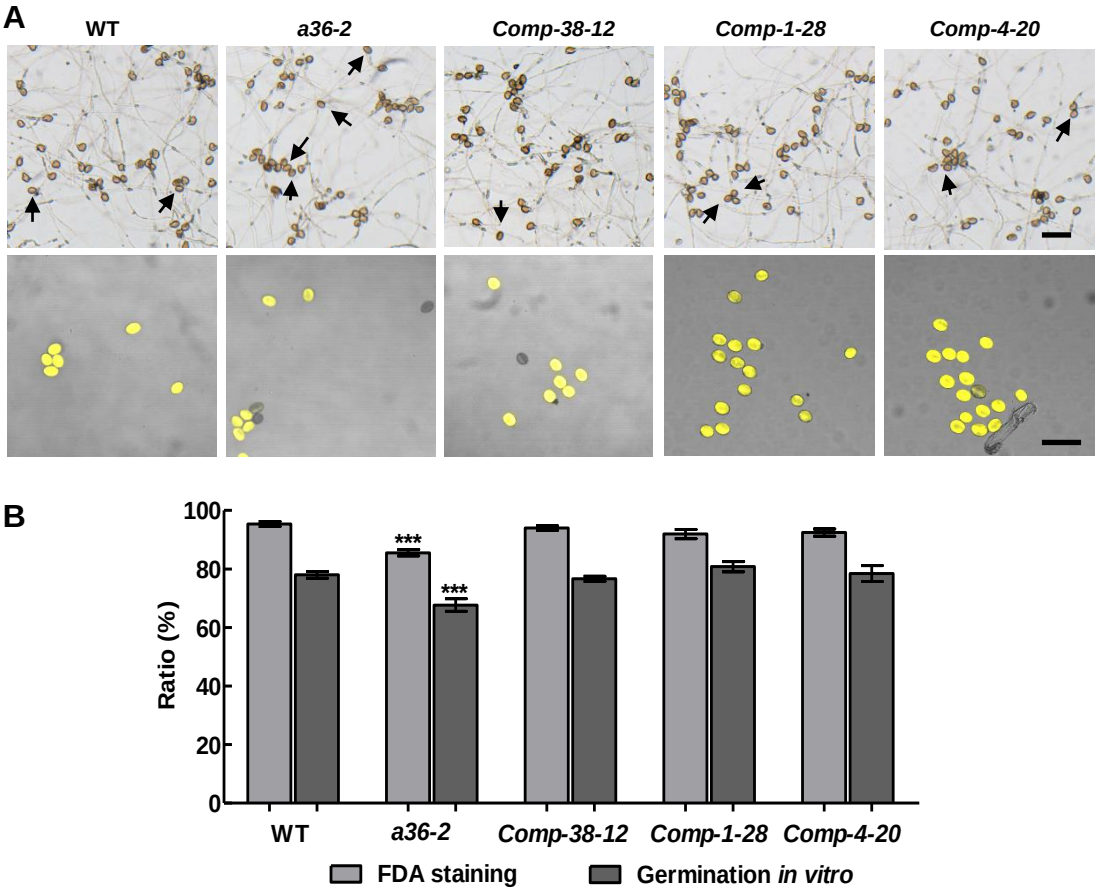

Supplemental Figure S9. Pollen germination ratio and pollen grain viability were recovered in the complemented *a36-2* mutant. A, Pollen germinated eight hours after incubation *in vitro* (top) and pollen viability by FDA staining (bottom) from wild-type, *a36-2* and complementary (*Comp*) plants (*pA36::A36/a36-2* transgenetic plants). Arrows designate ungerminated pollens, Bars = 100 μm. B, Statistical analysis of germination ratio and pollen viability ratio by FDA staining from wild-type, *a36-2,* complementary (*Comp*) plants (*pA36::A36/a36-2* transgenetic plants). Data were collected from three independent experiments (n > 300), the error bars show the standard error and an asterisk indicates values that significantly differ from those of the wild-type (****P* < *0.001*, calculated using Two-way ANOVA).

Supplemental Figure S10

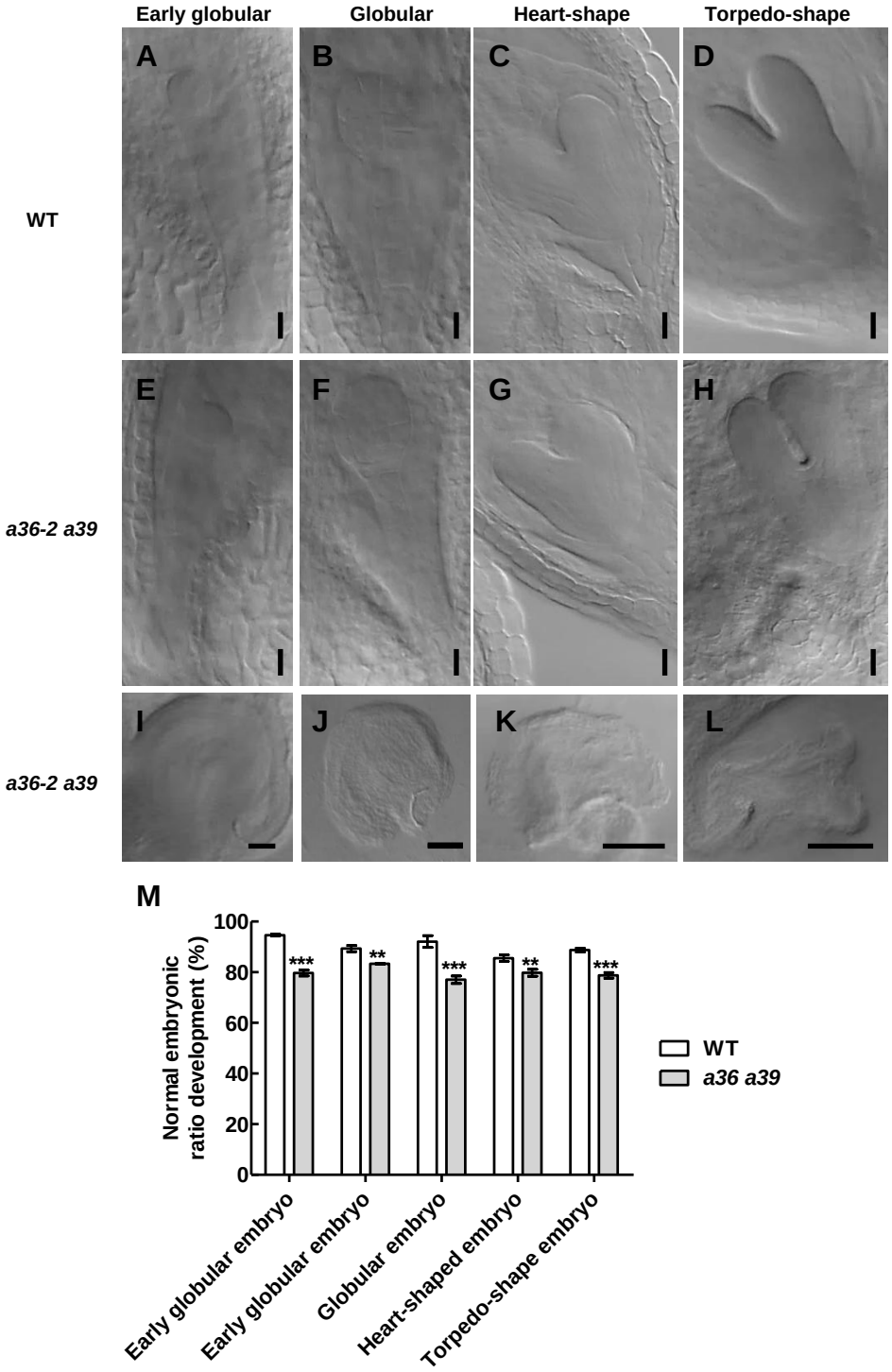

Supplemental Figure S10. Early embryo development in wild-type and *a36-2 a39*. A to D, Wild-type embryo show normal development from early globular embryo to torpedo-shape embryo. E to H, *a36-2 a39* embryo show normal development from early globular embryo to torpedo-shape embryo. I to L, Unfertilized ovules in the *a36-2 a39* pistil during different period of embryonic development. Bars = 20 μm. M, Statistical analysis of the normal embryonic development ratio. Data were collected from three independent experiments (n = 500), the error bars show the standard error ($^{**}P < 0.01$, $^{***}P < 0.001$, calculated using Two-way ANOVA).

Supplemental Figure S11

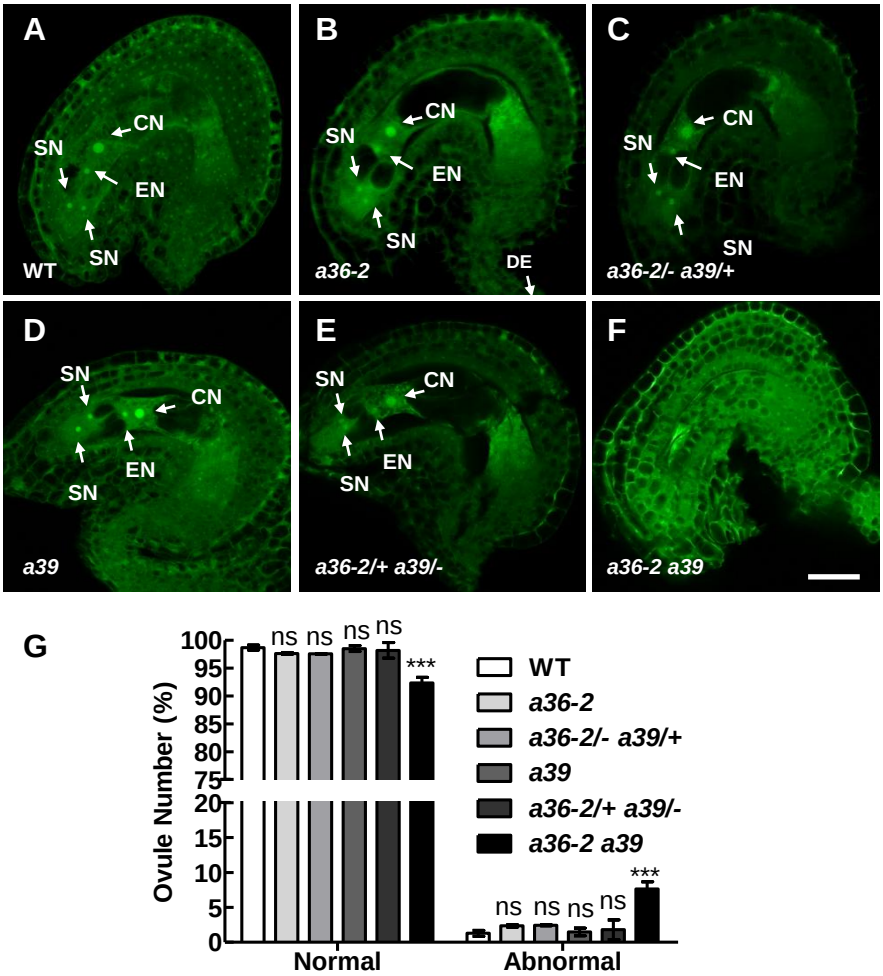

Supplemental Figure S11. CLSM analysis of ovules at FG7 in wild-type, *a36*, *a39*, and *trans*-heterozygous plants. An ovule with FG7 embryo sac in the wild-type (A), *a36-2* (B), *a36-2/- a39/+* (C), *a39* (D), *a36-2/+ a39/-* (E) and *a36-2 a39* (F), the embryo sac consists of two synergids nucleus (SN), the egg cell nucleus (EN), the large central cell nucleus (CN), the degenerated embryo sac (DE), Bars = 20 μm. G, Statistical analysis of the normal ovule (FG7) ratio. Data were collected from three independent experiments (n = 500), the error bars show the standard error (***$P < 0.001$, ns means no significant, calculated using Two-way ANOVA).

Supplemental Figure S12

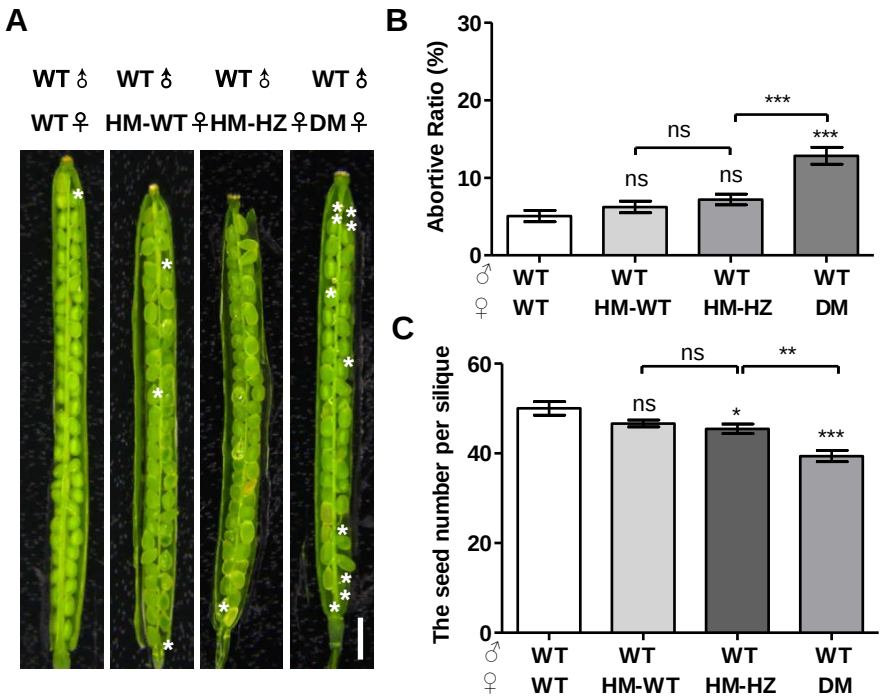

Supplemental Figure S12. Crosses among wild-type, *a36-2/- a39/+* and *a36 a39* plants. A, *In vivo* reciprocal cross-pollination of wild-type, HM-WT (*a36-2*), HM-HZ (*a36-2/- a39/+*) and DM (*a36-2 a39*) by wild-type pollens. Siliques were then dissected for examination of fertilized ovules. Asterisks designate unfertilized ovules in the silique. Bar = 1 mm. B, Statistical analysis of the abortive ratio of seed sets. The values are based on three biological replicates (n = 46 per cross). C, Statistical analysis of the seed number of mature siliques. The values are based on three biological replicates (n = 46 per cross). B and C, The error bars show the standard error and an asterisk indicates values that significantly differ from those of the wild-type (*$P < 0.05$, **$P < 0.01$,***$P < 0.001$, ns means no significant, calculated using Two-way ANOVA).

Supplemental Figure S13

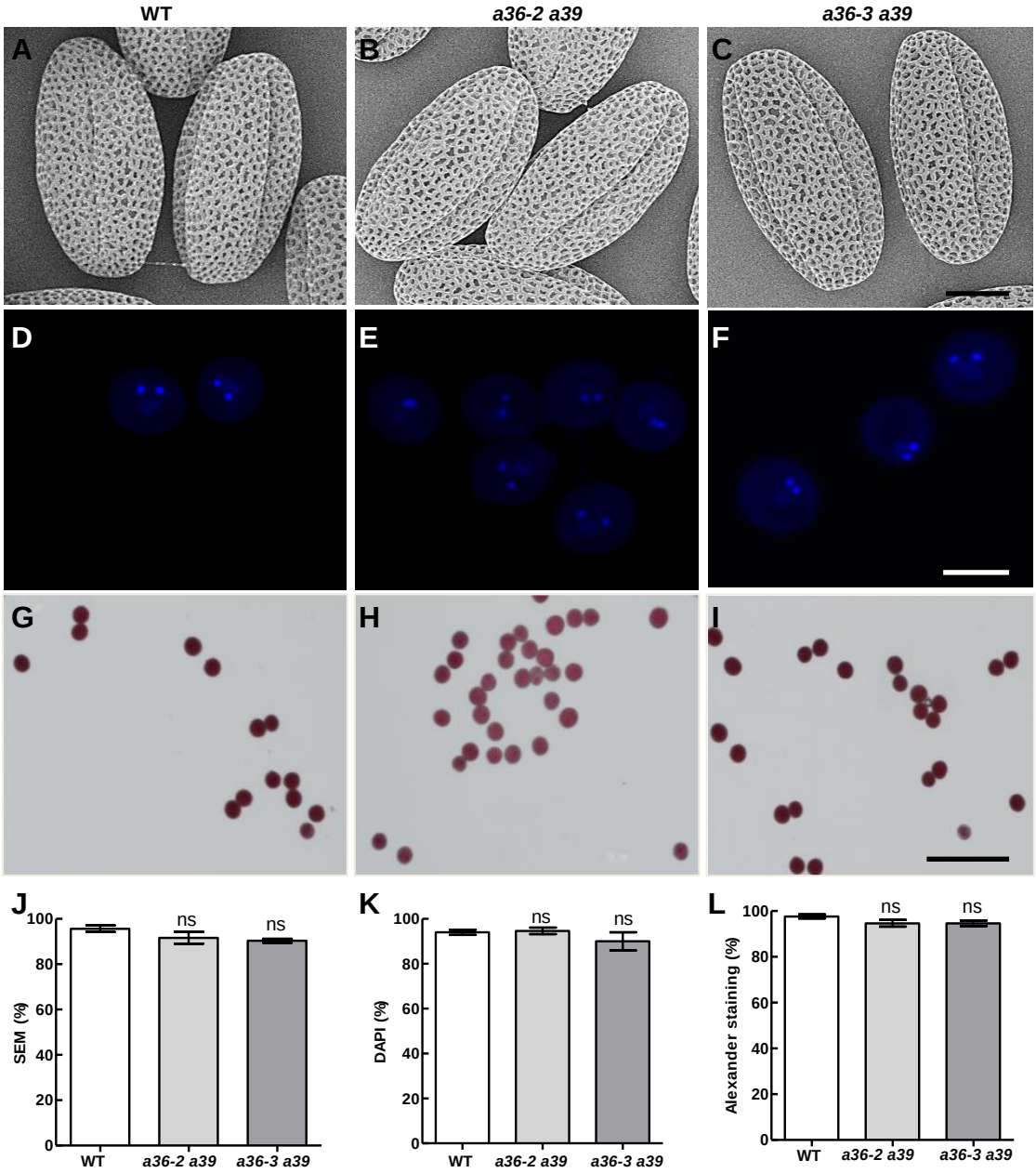

Supplemental Figure S13. Characterization of pollen grains in the *a36 a39* mutant. A to C, SEM image of wild-type (A), *a36-2 a39* (B), *a36-3 a39* (C) pollen grains, Bars = 10 μm. D to F, DAPI staining of pollen grains from wild-type (D), *a36-2 a39* (E), *a36-3 a39* (F) pollen grains, Bars = 50 μm. G to I, Alexander staining of wild-type (G), *a36-2 a39* (H), *a36-3 a39* (I) pollen grains, Bars = 100 μm. J, Statistical analysis of the normal pollen grains by SEM. K, Statistical analysis of the normal pollen grains by DAPI staining. L, Statistical analysis of the normal pollen grains by Alexander staining. Data were collected from three independent experiments (n > 300). The error bars show the standard error (ns means no significant, calculated using One-way ANOVA).

Supplemental Figure S14

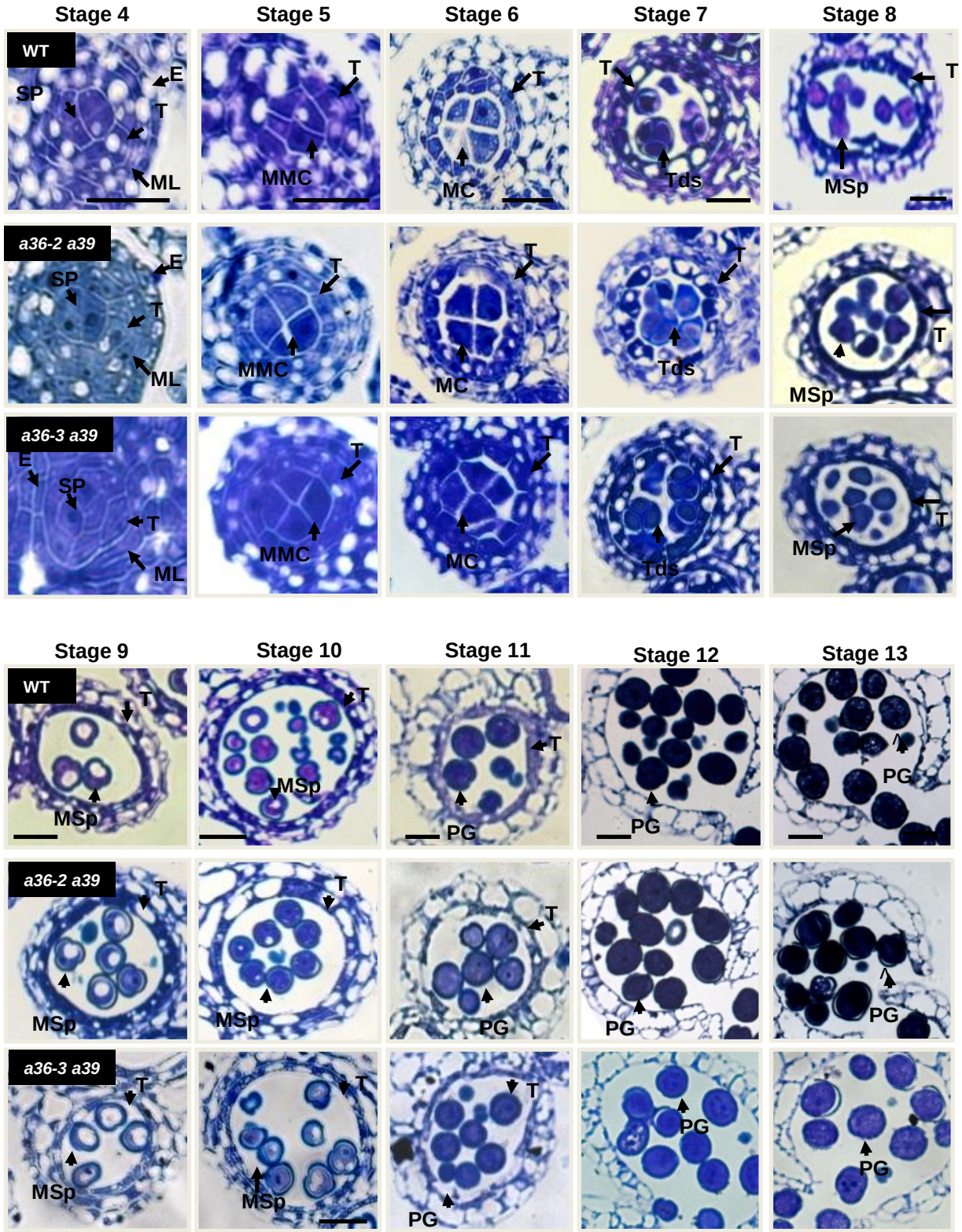

Supplemental Figure S14. Anther development of transverse section in wild-type and *a36 a39* double mutant. Ten different growth stages of anther development in the wild-type and the corresponding stages of development in the *a36 a39* double mutant were compared. The images are of cross sections through single locules. E, epidermis; ML, middle layer; T, tapetum; Tds, tetrads; Msp, microspore; SP, sporogenous cells; PG, pollen grains. Bars = 20 μm.

Supplemental Figure S15

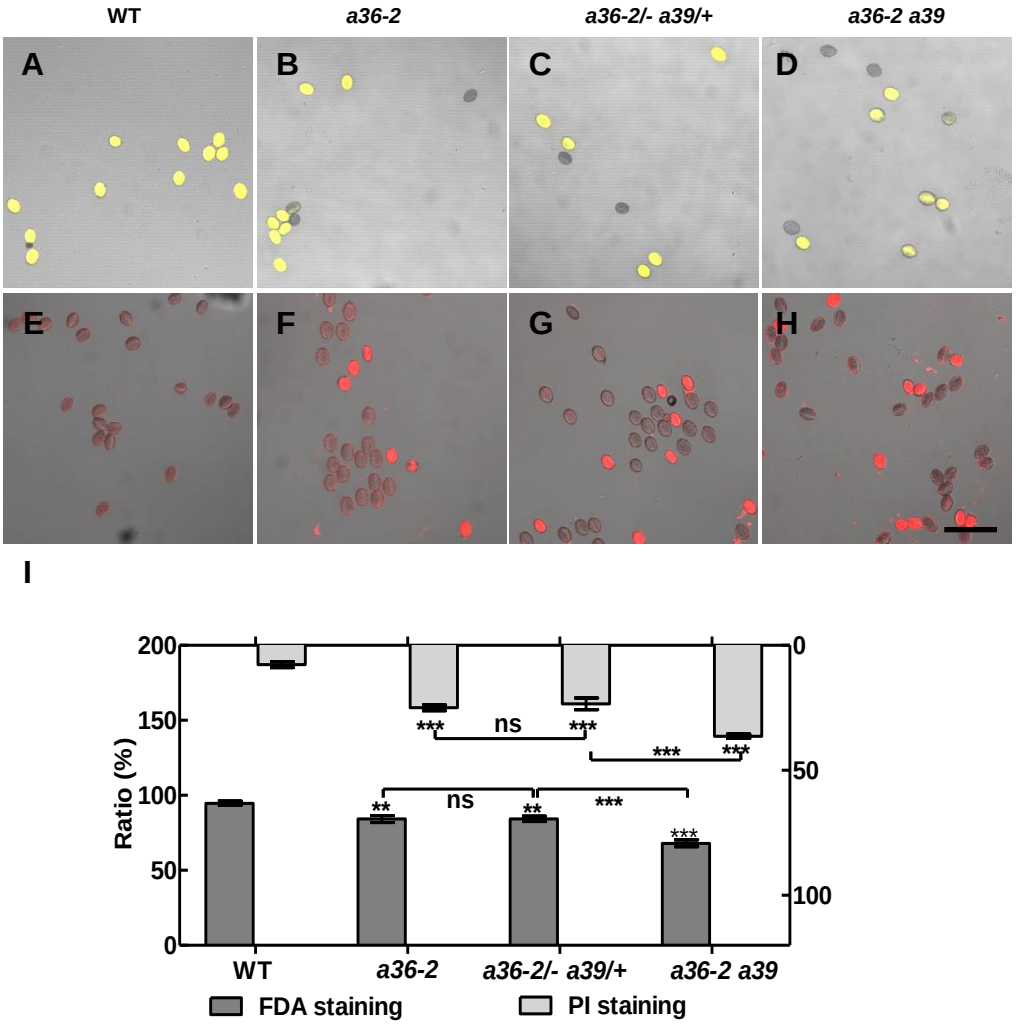

Supplemental Figure S15. *a36-2/- a39/+* displays reduced pollen grain activity *in vitro*. Pollen viability of wild-type (A, E), *a36-2* (B, F), *a36-2/- a39/+* (C, G), *a36 a39* (D, H) by FDA (top row) and PI (bottom row) staining. FDA positive (viable) and PI positive (unviable) pollen were indicated as yellow and red color, respectively. Bars = 100 μm. I, Statistical analysis of pollen viability by FDA and PI staining of pollen grains from wild-type, *a36-2*, *a36-2-/ a39/+*, *a36-2 a39* plants *in vitro*. Data were collected from three independent experiments (n > 900). The error bars show the standard error and an asterisk indicates values that significantly differ from those of the wild-type ($^{**}P < 0.01$, $^{***}P < 0.001$, ns means no significant, calculated using Two-way ANOVA).

Supplemental Figure S16

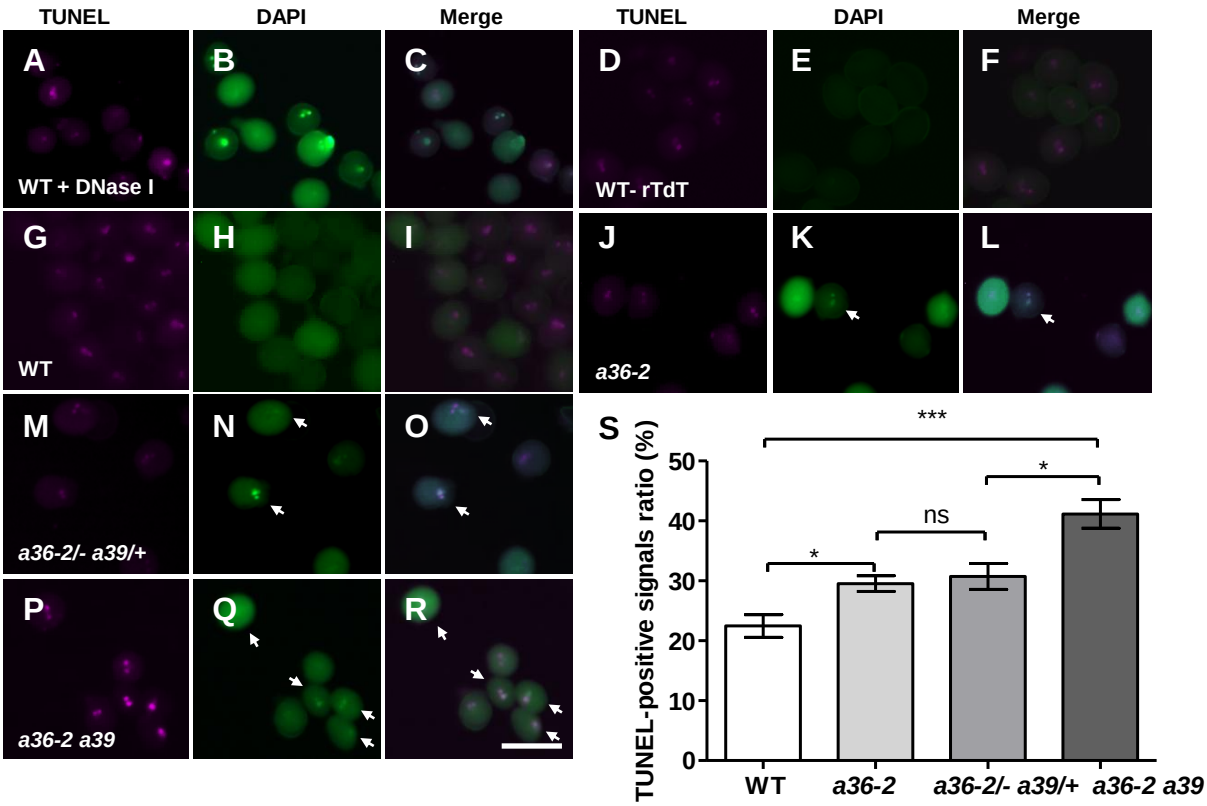

Supplemental Figure S16. TUNEL assay of mature pollen grains from wild-type, *a36-2*, *a36-2/- a39/+* and *a36-2 a39*. A to R, Fluorescence microscopy of DNA fragmentation detected using TUNEL assay of pollen grains in wild-type treated DNase I as positive control (A-C), wild-type treated without rTdT as negative control (D-F), wild-type (G-I), *a36-2* (J-L), *a36-2/- a39/+* (M-O) and *a36-2 a39* (P-R). Arrows in A to R indicate the TUNEL-positive signal in the pollen grains. Bar = 50 μm. S, Statistical analysis of TUNEL-positive signals ratio in wild-type, *a36-2*, *a36-2/- a39/+* and *a36-2 a39.* Data were collected from three independent experiments (n = 300). The error bars show the standard error and an asterisk indicates values that significantly differ from those of the wild-type (*$P < 0.05$, ***$P < 0.001$, ns means no significant, calculated using One-way ANOVA).

Supplemental Figure S17

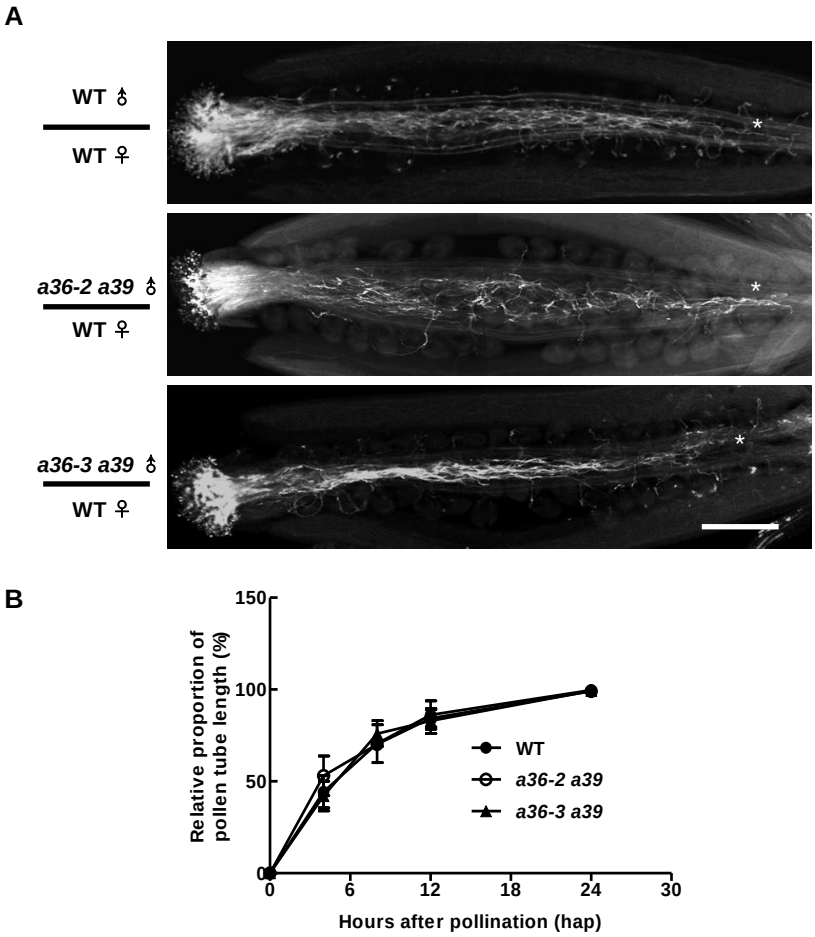

Supplemental Figure S17. Pollen tube growth of *a36 a39* mutants is normal in wild-type transmitting tract. A, Aniline blue staining of wild-type, *a36-2 a39* and *a36-3 a39* pollen about 12 hours after pollination on wild-type pistils . The asterisk shows the location of the pollen tube. Bars = 2 mm. B, Statistical analysis of different time points of pollen tube length. Data were collected from three independent experiments (n = 135), the error bars show the standard error (calculated using calculated Two-way ANOVA).

Supplemental Figure S18

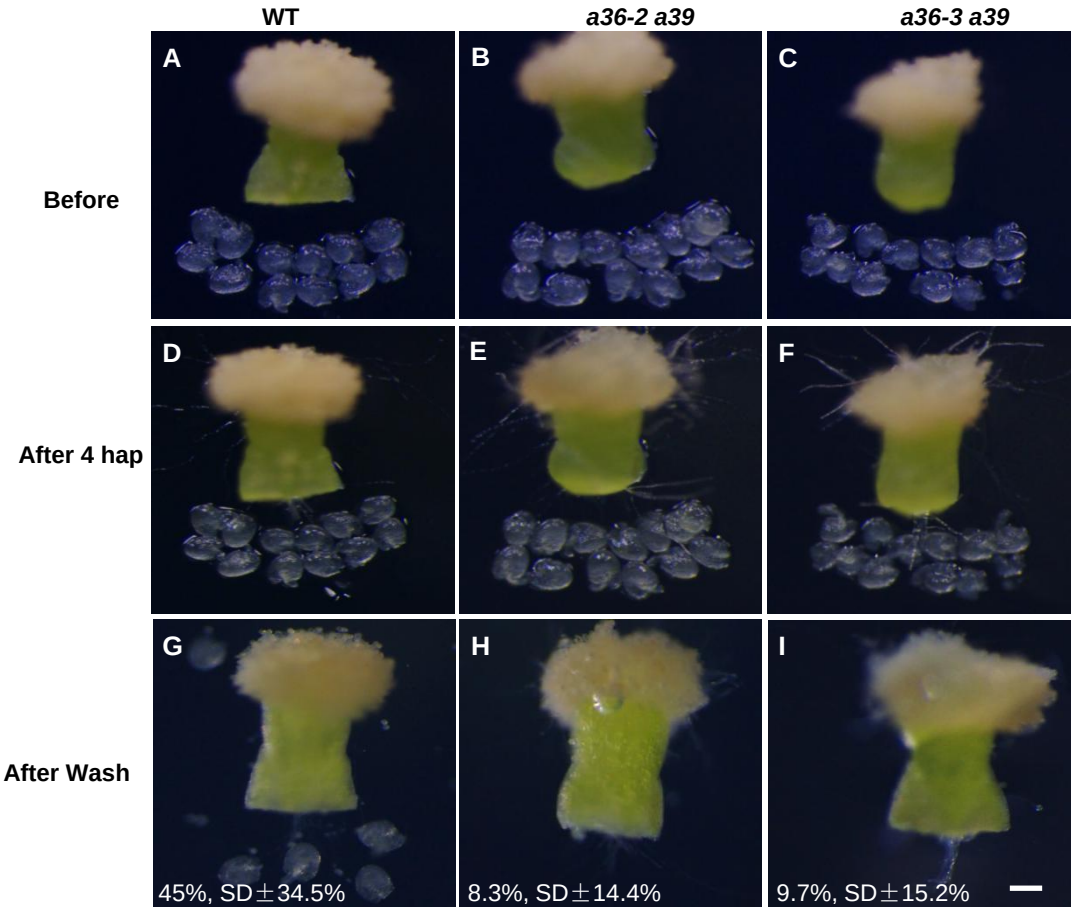

Supplemental Figure S18. Compromised directional growth of *a36 a39* pollen tubes in semi-*in vivo* pollination assay. About 12 ovules from unfertilized pistils were placed in front of cut ends of styles pollinated with either wild-type (A, D), *a36-2 a39* (B, E) or *a36-3 a39* (C, F) in each experiment. Untargeted ovules can float away while targeted ovules are connected by penetrating tubes after gentle washing. Each experiment was photographed before and after gentle washing for wild-type (A, D, G), *a36-2 a39* (B, E, H) and *a36-3 a39* (C, F, I). Targeting efficiency ratio is the number of targeted ovules to total ovules. Data were collected from three independent experiments (n = 120). Bar = 100 μm.

Supplemental Figure S19

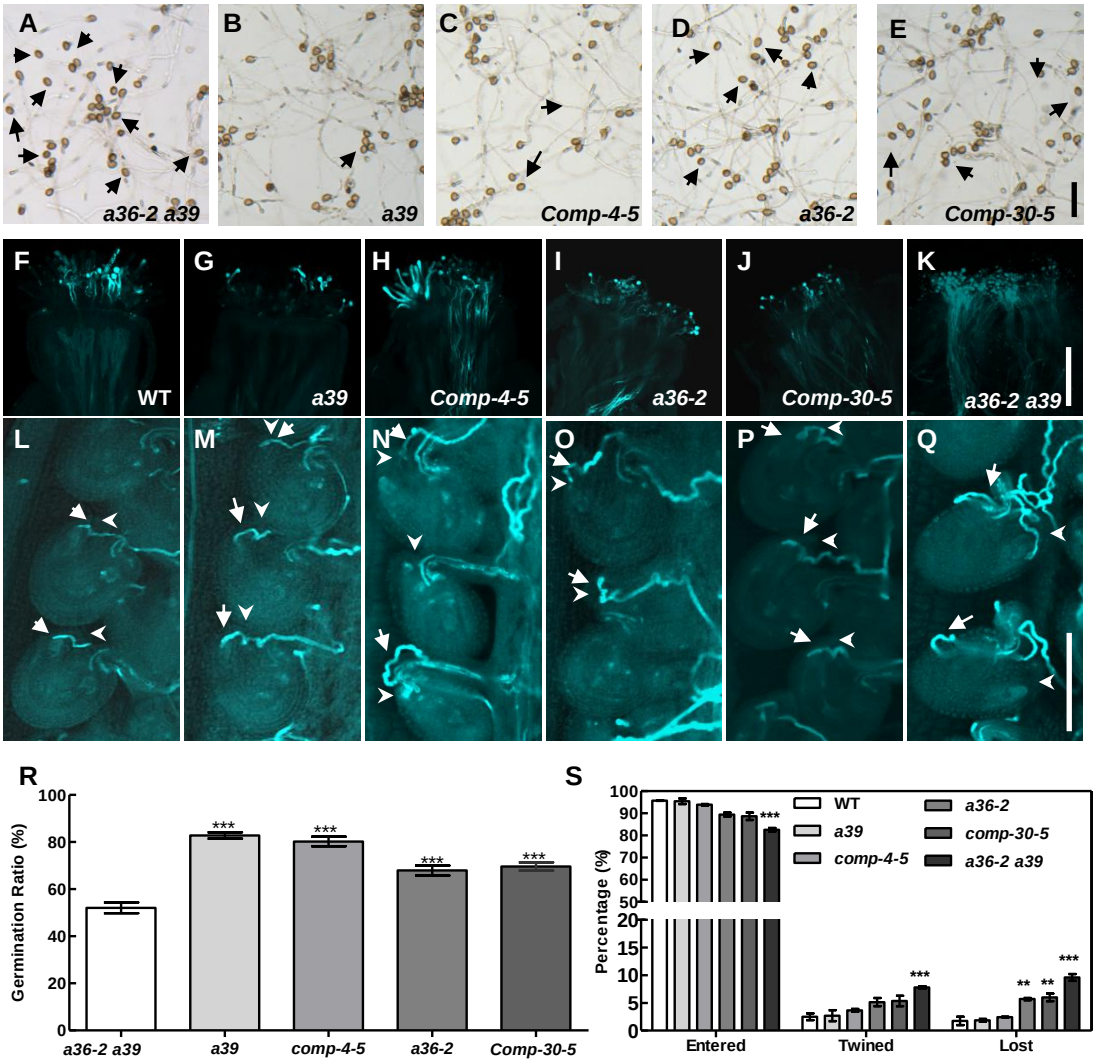

Supplemental Figure S19. The fragment of *A36*cDNA fused with GFP (*pA36:SP:GFP:A36cDNA*) and *A39*cDNA fused with GFP (*pA39:SP:GFP:A39cDNA*) could rescue the phenotype of *a36-2 a39.* A to E, Pollen germinated 8 hours after incubation *in vitro.* Germination of the pollen grains from *a36-2 a39* (A), *a39* (B), *pA36:SP:GFP:A36cDNA /a36-2 a39* transgenetic plants (C), *a36-2* (D) and *pA39:SP:GFP:A39cDNA/a36-2 a39* transgenetic plants (E), Arrows designate ungerminated pollens in A to E. Bar = 100 μm. Micropylar guidance of pollen tubes was recovered by the fragment of *A36*cDNA fused with GFP (*pA36:SP:GFP:A36cDNA*) and *A39*cDNA fused with GFP (*pA39:SP:GFP:A39cDNA*). F to Q, Directional growth of pollen tubes in wild-type (F), *a39* (G), *pA36:SP:GFP:A36cDNA/a36-2 a39* transgenetic plants (H), *a36-2* (I), *pA39:SP:GFP:A39cDNA/a36-2 a39* transgenetic plants (J) and *a36-2 a39* (K) in wild-type stigma and style with limited pollination condition. Bar = 200 μm. L to Q, The pollen tubes guidance of wild-type (L), *a39* (M), *pA36:SP:GFP:A36cDNA/a36-2 a39* transgenetic plants(N), *a36-2* (O), *pA39:SP:GFP:A39cDNA /a36-2 a39* transgenetic plants (P) and *a36-2 a39* (Q). Bar = 100 μm. R, Statistical analysis of germination rates after eight hours of pollen grains from *a36-2 a39*, *a39*, *pA36:SP:GFP:A36cDNA/a36-2 a39* transgenetic plants, *a36-2* and *pA39:SP:GFP:A39cDNA/a36-2 a39* transgenetic plants. Data were collected from three independent experiments (n > 300), the error bars show the standard error and an asterisk indicates values that significantly differ from those of the wild-type (***$P < 0.001$*, calculated using Two-way ANOVA). S, Statistical analysis of the different behaviors in pollen tubes with limited pollination. Arrows indicate the pollen tubes. Arrowhead indicates the micropyle. Data were collected from three independent experiments (n = 300), the error bars show the standard error and an asterisk indicates values that significantly differ from those of the wild-type (**$P < 0.01$, ***$P < 0.001$*, calculated using Two-way ANOVA).

Supplemental Figure S20

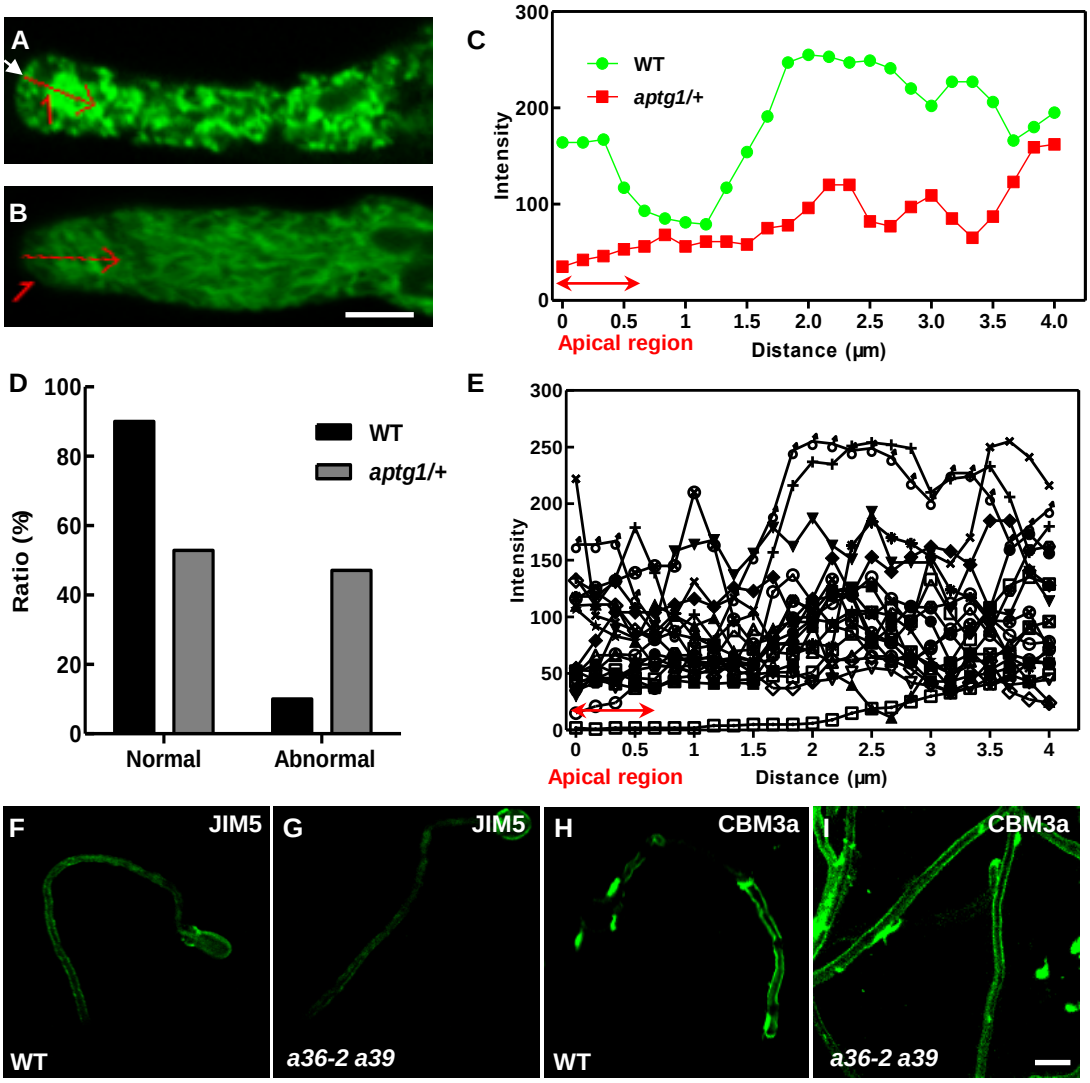

Supplemental Figure S20. Localization of A36-GFP in pollen tubes of the *aptg1/+* mutant and immnolabeling of cell wall polysaccharides in pollen tube of *a36-2 a39*. A, A36-GFP showing normal PM localization (arrow) in the tip of the wild-type pollen tube expressing *pA36:SP:GFP:A36cDNA*. B, A36-GFP showing abnormal localization (arrow) in the tip of the *aptg1/+* pollen tube expressing *pA36:SP:GFP:A36cDNA*. C, Fluorescence intensity through the red lines in the tips of pollen tubes showing normal (A) and abnormal (B) localization expressing A36-GFP in *aptg1/+*. D, Percentage of pollen tubes showing normal and abnormal localization of A36-GFP (n = 147) in the wild-type and the *aptg1/+* mutant. E, Fluorescence intensity of pollen tubes showing normal and abnormal localization of A36-GFP (n = 17) in the wild-type and the *aptg1* mutant. Bar = 5 μm. F and G, Immunofluorescence label was performed using JIM5 for de-esterified pectins. Wild-type tube (F) or *a36-2 a39* tube (G). H and I, Immunofluorescence labeling was performed using CBM3a for crystalline cellulose. Wild-type pollen tube (H) or *a36-2 a39* pollen tube (I). Representative tubes of three replicate experiments (n= 80,each experiment). Bar = 20 μm.

Supplemental Table Ⅰ. Primers for the identification of T-DNA insertion mutants

Primer name	Sequence	Purpose
A36-RT-FP	AATTCTCATCATCAGAAATACATAAAAC	For amplifying the endogenous transcript of *A36* in RT-PCR test
A36-RT-RP	TACAACAAAGAATGAGTAAGTTGTC	
A39-RT-FP	TTCGCAGGGAAGAAGAAGAAC	For amplifying the endogenous transcript of *A39* in RT-PCR test
A39-RT-RP	GAGGAGCCGATGAGAGATTG	
ACTIN7-F	AGGCACCTCTTAACCCTAAAGC	For amplifying the endogenous transcript of *AtACTIN7* in RT-PCR test as loading control group
ACTIN7-R	GGACAACGGAATCTCTCAGC	
T-DNA insertion-*a36-2*-F	TCCCAAGTGTCCTGTGAAAAC	For identifying the genotype of *a36-2* mutant plants
T-DNA insertion-*a36-2*-R	ATAGCGACCCTTGGTATCGAG	
LB2	GCTTCCTATTATATCTTCCCAAATTACCAATACA	
T-DNA insertion-*a36-3*-F	GAAACGCTTTATCTGTGCTGC	For identifying the genotype of *a36-3* mutant plants
T-DNA insertion-*a36-3*-R	GTTCGTTCATTATGCAATCCG	
LBb1.3	ATTTTGCCGATTTCGGAAC	

Supplemental Table Ⅱ. Primers used for constructions

Primer name	Sequence	Purpose
A36 genome-F1	AACTGCAGCTTTCTCTCCCATCTTTCAATCC	For amplifying the genomic DNA fragment in complementary assay
A36 genome-R1	CGATATTCGCAAGCATACGAG	
A36 genome-F2	TGACGCATAAGTTCGCCG	
A36 genome-R2	GCCCTGACTGATTTTTTCCAC	
A36 genome-F3	GTAGTGAATGCTGCTTCATCATAAG	
A36 genome-R3	GGGGTACCTGCCGTAGTTTGCCTATTCC	
A36 promoter-F	AACTGCAGCTTTCTCTCCCATCTTTCAATCC	For amplifying the native promoter fragment from genomic DNA for GUS staining
A36 promoter-R	TCCCCCGGGACCAAAACGAAAACCACCG	
A36 cDNA-F	TCCCCCGGGCGATTCACCATTTCAAACAAATC	For amplifying the cDNA fragment of *A36*
A36 cDNA-R	GGGGTACCCATGACCCAAAAAGCCAAAC	
GFP-A36-F	CGAGCTCATGGTGAGCAAGGGCGAG	For amplifying the GFP from *pCambia1300-Pro35S:GFPBS-2*
GFP-A36-R	CGAGCTCAAGATCTACCATGTACAGCTCGTCC	
A39 promoter-F	AACTGCAGGTTTGACCTGAAGAAAGAGAAGAAG	For amplifying the native promoter fragment from genomic DNA for GUS staining
A39 promoter-R	TCCCCCGGGGAGATCAATGGAAGCGAGCAT	
A39 cDNA-F	CAAGTTCGCAGGGAAGAAGAAG	For amplifying the cDNA fragment of *A39*
A39 cDNA-R	TCCCCCGGGAGCATCCATCACCAAGACAATG	
GFP-A39-F	CCGCTCGAGATGGTGAGCAAGGGCGAG	For amplifying the GFP from *pCambia1300-Pro35S:GFPBS-2*
GFP-A39-R	CCGCTCGAGAAGATCTACCATGTACAGCTCGTCC	
A36-F	GGAATTCATGGTGACGACGATGGATC	For expression of A36 fusion protein *in E. coli*
A36-R	CCGCTCGAGCTATGAAGTAAAAGAATGGAAAACC	
A36-D-F	GGAATTCAAGTTCGCCGGAAAAGAG	For expression of A36 domain fusion protein *in E. coli*
A36-D-R	CCGCTCGAGTTAGAGTTGGTAAGCCGCTCCT	
A39-F	GGAATTCATGGAACTGAGGAGAAAATTGTGC	For expression of A39 fusion protein *in E. coli*
A39-R	GCGTCGACCTATGCTAAGGAAGTAAAAGCCATTACG	
A39-D-F	GGAATTCCAACACAAGTTCGCAGGGAAG	For expression of A39 domain protein *in E. coli*
A39-D-R	GCGTCGACGTTATGATCTGCCCATCCGATCAC	